

Reduced Surface Sidewall Recombination and Diffusion in Quantum-Dot Lasers

Stephen A. Moore, Liam O'Faolain, Maria Ana Cataluna, Michael B. Flynn, Maria V. Kotlyar, and Thomas F. Krauss

Abstract—We examine the surface recombination rate in quantum-dot semiconductor lasers and determine the diffusion length (1.0 μm) and, for the first time, provide a value for surface recombination velocity (5×10^4 cm/s) in quantum-dot material. As a result of strong carrier confinement in the dots, these values are much lower than in comparable quantum-well lasers (5×10^5 cm/s and 5 μm , respectively) allowing the creation of narrow (2–3 μm wide) lasers with comparable threshold currents to those of broad area devices.

Index Terms—Diffusion length, low threshold, quantum-dot lasers, surface recombination.

I. INTRODUCTION

QUANTUM-DOT lasers have received considerable interest in recent years due to their potential for temperature-independent operation, low linewidth enhancement factors, low threshold currents, resistance to optical feedback, and ability to provide gain at the telecommunication wavelengths from a GaAs-based material.

In narrow mesa quantum-well lasers, surface recombination at the etched sidewalls can be a major factor affecting the performance of the device. Where the lattice abruptly terminates, “dangling bonds” are formed, creating surface states through which carriers may recombine nonradiatively. This process may be characterized by a surface recombination velocity v_s . Values of order 10^5 – 10^6 cm/s⁻¹ are typical for GaAs and 10^4 cm/s⁻¹ for InP [1]. This can severely compromise device performance.

Recent works [2], [3] have observed that sidewall recombination in quantum-dot lasers is much reduced compared to that in quantum wells, though without fully characterizing this behavior. The reduction may be attributed to the strong three-dimensional confinement of carriers to the dots. Carriers that are trapped in a dot do not interact with any defects; only while they are in the wetting layer may diffusion to a recombination center take place. This effectively reduces the diffusion length, as due to continual trapping by and escaping from the dots (due to thermal effects), the freedom of the carrier is greatly restricted.

In this letter, we examine the phenomenon in detail and quantify the parameters that dominate its behavior.

Manuscript received March 22, 2006; revised May 18, 2006. The work of M. A. Cataluna was supported in part by FCT—Fundação para a Ciência e Tecnologia, Portugal, through scholarship SFRH/BD/10879/2002.

S. A. Moore, L. O'Faolain, M. B. Flynn, M. V. Kotlyar, and T. F. Krauss are with the Department of Physics and Astronomy, University of St. Andrews, St. Andrews, Fife KY16 9SS, U.K. (e-mail: sam15@st-andrews.ac.uk).

M. A. Cataluna is with Department of Physics and Astronomy, University of St. Andrews, St. Andrews, Fife KY16 9SS, U.K., and also with the GoLP/Centro de Fisica de Plasmas, Instituto Superior Tecnico, 1049-001 Lisbon, Portugal.

Digital Object Identifier 10.1109/LPT.2006.881206

II. PROCEDURE

A material consisting of ten layers of InAs quantum dots inside Ga_{0.85}In_{0.15}As quantum wells was grown by NL Nanosemiconductor GmbH using molecular beam epitaxy. The size and composition of the dots was chosen such that the peak of emission was at 1280 nm. Initially, broad area lasers (50 μm wide), of varying length, were fabricated to determine the material constants [4].

Using electron beam lithography, 2–10- μm -wide stripes were defined and then transferred into a hydrogen silsesquioxane (HSQ) hard mask (baked at 500 °C for one hour) [5] using reactive ion etching (fluorine chemistry). The 2.2- μm -high mesas were etched using a high beam voltage/low beam current regime of chemically assisted ion beam etching [6]. The remaining HSQ was then removed with hydrofluoric acid.

Self-aligned BCB insulation pads were created using an etch-back technique. Electrical contacts were deposited using electron beam evaporation.

Broad area (50 μm) and varied width (5–50 μm wide) mesa lasers were also created in a quantum-well material. This was a double quantum-well design, emitting at 980 nm, grown at the University of Sheffield. The fabrication process was the same as that for the quantum-dot devices.

The samples were cleaved into chips of suitable length (approximately 2 mm for the quantum-dot and 0.6 mm for the quantum-well devices) and mounted p-side up on copper blocks. Power-current curves were then obtained for each laser and a curve of threshold current density against mesa width obtained for both materials. For a 5- μm -wide 2-mm-long quantum-dot device, the threshold current was measured as 140 Acm⁻², comparing favorably with that of a similar length broad area device (122 Acm⁻²).

The passive optical loss of each waveguide was measured by taking a transmission spectrum using a tunable laser in the wavelength range of 1300–1310 nm. The internal loss α_i was determined from the Fourier transform of the resulting Fabry–Pérot oscillations [7]. A loss value of 5 cm⁻¹ for the quantum-dot devices was obtained that, within experimental error, was identical for all waveguides, indicating that the dependence of threshold current density on ridge width is dominated by sidewall recombination effects rather than by optical losses.

III. ANALYSIS AND RESULTS

A simple theoretical model was used to fit the experimental results and establish values of v_s , following the approach of Coldren *et al.* [8]. The model was constructed by consideration

of the transverse carrier density $N(x)$. Starting from the simple lateral diffusion equation

$$D \frac{d^2 N(x)}{dx^2} = -\frac{\eta_i J(x)}{qd} + \frac{N(x)}{\tau} \quad (1)$$

where D is the diffusion coefficient, η_i is the injection efficiency (taken to be 0.7 for the quantum wells and the quantum dots), $J(x)$ is the applied current density assumed to be invariant in the x direction ($J(x) = J_0$), q is the electronic charge, d is the depth of the active region, and τ is the carrier lifetime (taken to be 2 ns in the wells [9] and 2.8 ns in the dots [10]). Equation (1) can be solved analytically at threshold ($J(x) = J_{th}$), with the boundary conditions that $dN/dx = 0$ at the ridge center ($x = 0$) (from symmetry) and that the diffusion current DdN/dx is equal to the surface recombination current $-v_s N$ at the ridge edge ($x = W/2$), giving the expression

$$N_{th}(x) = A \cosh\left(\frac{x}{L_d}\right) + N_p \quad (2)$$

with

$$N_p = \frac{\eta_i J_{th} \tau}{qd} \quad (3)$$

and

$$A = -v_s N_p \left[\frac{D}{L_d} \sinh\left(\frac{W}{2L_d}\right) + v_s \cosh\left(\frac{W}{2L_d}\right) \right]^{-1} \quad (4)$$

where L_d is the diffusion length, equal to $(D\tau)^{0.5}$, and is used as a fitting parameter in the model, N_p is the injected carrier density, and J_{th} is the threshold current density. The 50- μm -wide varied length laser data was used to model the variation of threshold gain G with threshold carrier density. For a 50- μm -wide device, we can assume $N_{th} \approx N_p$. The threshold gain was calculated by setting it equal to the optical losses

$$G = \frac{(\alpha_i + \alpha_m)}{\Gamma_x \Gamma_z} \quad (5)$$

with

$$\Gamma_x = \gamma \left[2 \left(\frac{n_{eff2}}{n_{eff1}} \right)^4 + \gamma \right]^{-1} \quad (6)$$

and

$$\gamma = 4\pi^2 W^2 \lambda^{-2} (n_{eff2}^2 - n_{eff1}^2) \quad (7)$$

where α_i is taken to be 11 cm^{-1} for the wells and 5 cm^{-1} for the dots, α_m is the mirror loss equal to $\ln(1/R)/L$, where R is the facet reflectivity taken to be 0.33 and L is the device length. Γ_x is the lateral confinement, Γ_z is the vertical confinement taken to be 0.05 for the wells and 0.016 for the dots and λ is the freespace wavelength. n_{eff} is the effective refractive index for the given material, calculated to be 3.23 for the wells and 3.43 for the dots using a commercial eigenmode solver (FIMMWAVE). Fig. 1 shows the variation of G with N_{th} using the data for the 50- μm -wide quantum-dot lasers. As the lasers are operating below saturation, this plot can be modelled by the logarithmic expression

$$G(N_{th}) = g_0 \ln\left(\frac{N_{th}}{N_{tr}}\right) \quad (8)$$

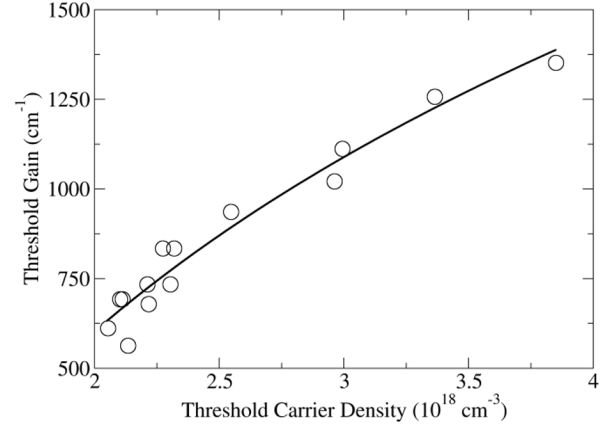


Fig. 1. Variation of threshold gain with Threshold Carrier Density for 50- μm -wide quantum-dot lasers.

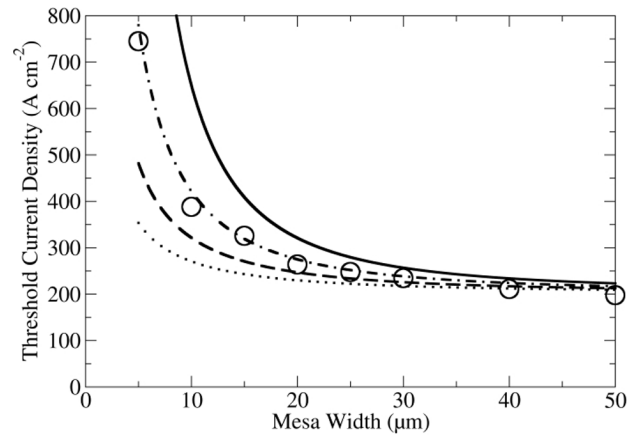


Fig. 2. The theoretical dependence of the threshold current density on mesa width for quantum-well lasers. The experimental data is overlaid. The solid, dash-dot, dash and dot represent values of v_s of 5×10^6 , 5×10^5 , 2×10^5 and 1×10^5 cm/s^{-1} respectively.

where g_0 is the gain cross section at transparency (found to be 720 and 1199 cm^{-1} in the wells and dots, respectively) and N_{tr} is the carrier density at transparency (found to be 6.85×10^{17} and 1.21×10^{18} cm^{-3} in the wells and dots, respectively). As G is a function of ridge width W , we can rearrange (8) to obtain $N_{th}(W)$. For narrow ridges, the assumption $N_{th} \approx N_p$ is no longer valid. We therefore have to integrate (2) across the mesa to obtain an effective carrier density N_{eff} . This integration also needs a weighting function $P(x)$ to account for the mode profile. $P(x)$ was approximated as a normalized cosine function $(\pi/2W) \cos(\pi x/W)$ as this is the form of a fundamental waveguide mode inside a mesa. The resultant integral gives

$$N_{eff} = \frac{A\pi^2 L_d^2 \cosh\left(\frac{W}{2L_d}\right)}{\pi^2 L_d^2 + W^2} + N_p. \quad (9)$$

N_{eff} can be substituted for N_{th} in (8) and solved for $N_p(W)$ and subsequently $J_{th}(W)$. The theoretical plot of $J_{th}(W)$ for the quantum-well devices, along with the experimental results are plotted in Fig. 2. From the plot $v_s \sim 5 \times 10^5$ cm/s^{-1} which is in good agreement with accepted values [8], giving us confidence in the model. A value of 5 μm for L_d provided the best fit. $J_{th}(w)$ for the quantum-dot devices, along with the

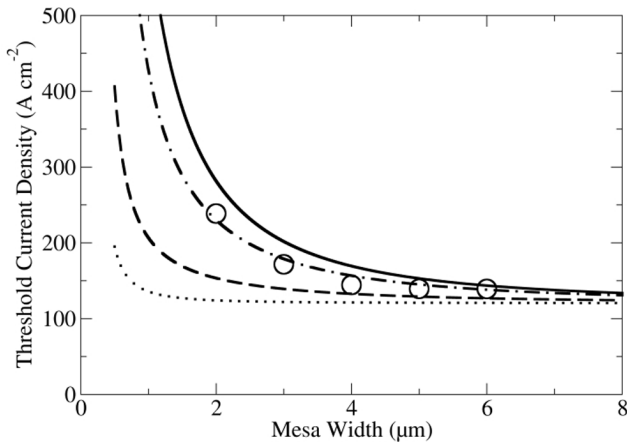


Fig. 3. The theoretical dependence of the threshold current density on mesa width for quantum-dot lasers. The experimental data is overlaid. The solid, dash-dot, dash and dot represent values of v_s of 1×10^5 , 5×10^4 , 1×10^4 and 0 cm/s^{-1} respectively.

experimental results is plotted in Fig. 3. From the plot $v_s \sim 5 \times 10^4 \text{ cm/s}^{-1}$ in the quantum-dot devices. A value of $1.0 \mu\text{m}$ for L_d in the dots provided the best fit. This value shows good agreement with that measured by Popescu *et al.* [11]. Of the key constants (τ , α_i , η_i , Γ_z), only a variation in τ ($\pm 25\%$) clearly affected the extracted results, causing a small change in L_d ($\pm 10\%$). This shows that the measurement is tolerant to any inaccuracies in the unmeasured constants.

IV. CONCLUSION

For the first time, we have fully characterized surface recombination in a quantum-dot material, uniquely measuring both the surface recombination velocity ($5 \times 10^4 \text{ cm/s}$) and the diffusion length ($1.0 \mu\text{m}$). Both these parameters are necessary for a full understanding. The order of magnitude difference in surface recombination and the reduced diffusion length between quantum wells and quantum dots allows the creation of high-performance, narrow quantum-dot mesa lasers. The consequent strong confinement of carriers to the active layer (with little penalty due to surface recombination) means that these devices are very efficient with threshold current densities comparable to those of broad area lasers. The prevention of current spreading may also be expected to improve the high-frequency performance of these devices through a reduction in the parasitic capacitance [3]. The large refractive index contrast, due to the mesa structure, also provides high optical confinement which considerably extends the range of available cavity geometries, allowing, for example, ring lasers with tighter bending radii. Additionally, the reduced value of v_s potentially allows the creation

of GaAs-based photonic crystal lasers—devices that were previously inefficient due to the high value of v_s in quantum wells. Furthermore, a lower value of v_s should be obtainable by optimization of the fabrication conditions, such as the CAIBE etch step that may generate excess damage at the sidewalls [12].

ACKNOWLEDGMENT

The authors would like to thank G. Robb for his help with experiments and Dr. D. O'Brien for useful discussions and suggestions.

REFERENCES

- [1] M. Boroditsky, I. Gontijo, M. Jackson, R. Vrijen, E. Yablonovitch, T. Krauss, C.-C. Cheng, A. Scherer, R. Bhat, and M. Krames, "Surface recombination measurements on iii-v candidate materials for nanostructure light-emitting diodes," *J. Appl. Phys.*, vol. 87, no. 7, pp. 3497–3504, Apr. 2000.
- [2] D. Ouyang, N. N. Ledentsov, D. Bimberg, A. V. Kovsh, A. E. Zhukov, S. S. Mikhlin, and V. M. Ustinov, "High performance narrow stripe quantum-dot lasers with etched waveguide," *Semiconductor Sci. Tech.*, vol. 18, no. L53, Dec. 2003.
- [3] M. Kuntz, M. Lammlin, D. Bimberg, M. G. Thompson, K. T. Tan, C. Marinelli, R. V. Penty, I. H. White, V. M. Ustinov, A. E. Zhukov, Y. M. Shernyakov, and A. R. Kovsh, "35 GHz mode-locking of $1.3 \mu\text{m}$ quantum dot lasers," *Appl. Phys. Lett.*, vol. 85, no. 5, pp. 843–845, Aug. 2004.
- [4] P. McIlroy, A. Kurobe, and Y. Uematsu, "Analysis and application of theoretical gain curves to the design of multi-quantum-well lasers," *IEEE J. Quantum. Electron.*, vol. 21, no. 12, pp. 1958–1963, Dec. 1985.
- [5] L. O'Faolain, M. V. Kotlyar, N. Tripathi, R. Wilson, and T. F. Krauss, "Fabrication of photonic crystals using a spin-coated hydrogen silsesquioxane hard mask," *J. Vac. Sci. Technol. B*, vol. 24, no. 1, pp. 336–339, Jan. 2006.
- [6] M. V. Kotlyar, L. O'Faolain, R. Wilson, and T. F. Krauss, "High-aspect-ratio chemically assisted ion-beam etching for photonic crystals using a high beam voltage-current ration," *J. Vac. Sci. Technol. B*, vol. 22, no. 4, pp. 1788–1791, Jul. 2004.
- [7] M. V. Kotlyar, T. Karle, M. D. Settle, L. O'Faolain, and T. F. Krauss, "Low-loss photonic crystal defect waveguides in InP," *Appl. Phys. Lett.*, vol. 84, no. 18, pp. 3588–3590, May 2004.
- [8] L. A. Coldren and S. W. Corzine, *Diode Lasers and Photonic Integrated Circuits*. New York: Wiley, 1995.
- [9] H. Hillmer, A. Forchel, S. Hansmann, M. Morohashi, E. Lopez, H. P. Meier, and K. Ploog, "Optical investigations on the mobility of two-dimensional excitons in GaAs/GaAlAs quantum wells," *Phys. Rev. B*, vol. 39, no. 15, pp. 10901–10912, May 1989.
- [10] M. Sugawara, K. Mukai, Y. Nakata, H. Ishikawa, and A. Sakamoto, "Effect of homogeneous broadening of optical gain on lasing spectra in self-assembled InGaAs quantum dot lasers," *Phys. Rev. B*, vol. 61, no. 11, pp. 7595–7603, Mar. 2000.
- [11] D. P. Popescu, P. G. Eliseev, A. Stintz, and K. J. Malloy, "Carrier migration in structures with InAs quantum dots," *J. Appl. Phys.*, vol. 94, no. 4, pp. 2454–2458, Aug. 2003.
- [12] J. Daleiden, R. Kiefer, S. Klussmann, M. Kunzer, C. Manz, M. Wailher, J. Braunstein, and G. Weimann, "Chemically-assisted ion-beam etching of (AlGa)As/GaAs: Lattice damage and removal by *in situ* cl-2 treatment," *Micro. Eng.*, vol. 45, no. 1, pp. 9–14, Feb. 1999.